Brain Structures Segmentation using Optimum Global and Local Weights on Mixing Active Contours and Neighboring Constraints

Dimitrios Zarpalas[1,2]
zarpalas@iti.gr

Anastasios Zafeiropoulos[1]
zafeirop@iti.gr

Petros Daras[1]
daras@iti.gr

Nicos Maglaveras[2]
nicmag@med.auth.gr

Michael G. Strintzis[1]
michael@iti.gr

[1]Informatics and Telematics Institute, Centre for Research and Technology Hellas, 57001 Greece
[2]Laboratory of Medical Informatics, Medical School, Aristotle University of Thessaloniki, 54124 Greece

ABSTRACT

This paper presents a new method for segmenting multiple brain structures by using an optimized mixture of different Active Contour Models (ACMs). Prior constraints and structures' neighboring interaction are modelled for each structure. Prior information is also captured by a training process, in which structure's dependent local and global weights are calculated. The local weights regulate locally the combination of each term during the evolution, acting as an experienced balancer between image and prior information. The ideal proportion of relation between the mixture of different ACMs and the prior model is defined by the optimum global weights. As proof of concept, the method is applied on the very challenging task of segmenting hippocampus and amygdala structures.

Categories and Subject Descriptors

I.4.6 [**Image Processing**]: Segmentation—*Region growing, partitioning*, [Edge and feature detection]; I.5.4 [**Pattern Recognition**]: Applications—*Computer Vision*; J.3 [**Life and Medical Sciences**]: [Medical information systems]

General Terms

Algorithms, Experimentation and Theory.

Keywords

Medical imaging, brain MRI segmentation, hippocampus-amygdala segmentation, region-based and gradient-based active contours, prior knowledge, gradient distribution on boundaries.

1. INTRODUCTION

Brain segmentation of anatomical structures is an emerging field of research with important applications. Information about anatomical structures can be extracted and further analyzed for clinical and medical research purposes. Although the large amount of effort invested on the topic, it still continues to challenge researchers for seeking more accurate results.

Boundaries among brain structures are often not clear, while intensity and texture patterns of different structures are quite similar, leading to inaccurate segmentation results. The hippocampus and amygdala case is one of the most challenging, due to unclear, or even missing, boundaries between them, and other surrounding regions, as figure 1 shows.

Various methods have been proposed on this task, with a significant amount of them being with deformable models. ACMs deform a contour in accordance to image information based on image gradient [1] or gray-level intensity statistical information [2]. These two main types are well known as region-based or edge-based methods. Region-based methods for ACMs utilize intensity statistical information of the image to control the contour and grow it to homogeneous regions.

Many efforts have been devoted in prior knowledge utilization into the existing frameworks to improve medical image segmentation accuracy. Cootes *et al.* [3] made a breakthrough by constructing shape models from statistical analysis based on corresponding points across a set of images. Leventon [7] introduced the idea of incorporating shape analysis into the level-set functions through distance maps and perform Principal Component Analysis (PCA) on level-set functions. Davatzikos *et al.* [4] further proposed wavelet analysis on the coordinates of the structure's boundaries, reducing significantly the size of the required training set.

Since then, remarkable work has been conducted on multiphase and multiple structure segmentation utilizing both shape prior methods and image features. Yang *et al.* [13] studied the variational relations of neighboring objects and the contour was evolving both according to image gray information and neighbor prior information. However, contours were evolving independently making it very difficult to control the overlap problem. A similar approach was developed in [11], [8]. To overcome these problems, *Yan et al.* [12]

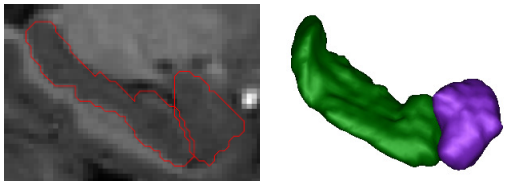

Figure 1: Illustration of a slice from a brain MRI. Colored contours depict outer boundaries of the hippocampus and amygdala structures, produced by manual segmentation. On the right, 3D reconstructions of the two structures.

proposed a repulsive term in order to isolate the structures and prevent segmentation overlapping.

The aforementioned related work, assumes that the combination of the gray-level image information and the prior knowledge should be mixed in energy functionals, through global multiplicative weights. In this manner, regions with high gradients are affected from prior knowledge in the same degree with regions of weak boundaries. Furthermore, prior information is applied symmetrically to the complete image domain, while only some regions actually require this knowledge.

Extending previous work on the gradient distribution on hippocampus boundary in [14], this work presents a multi-structure segmentation framework in which each structure's prior knowledge is combined with image information. A local weighting scheme, encapsulates knowledge of the extend to which one should trust the image information or the prior knowledge for any specific point in the image. This local scheme, called Gradient Distribution of Boundaries (GDB), acts at voxel level and controls contour evolution as a local balancer: in image regions with evident boundaries and strong edges, the ACM should evolve based on image statistic or gradient information, while in regions with unclear or missing boundaries, prior information should take control of the evolution. Acting this way, GDB tries to mimic human's visual perception of segmenting ambiguous images, based on prior knowledge of the scene. To further improve robustness and take advantage of benefits of both types of image term based evolution, the region-based framework is mixed with the edge-based. The edge-based model will contribute to boundary regions with high gradient, while the region-based model will support in noisy areas with weaker boundaries. In an effort to optimally balance the mixture model per structure, because different structures follow different boundary patterns, global weights are incorporated to each of the including terms, and are found for each structure separately in a single framework.

2. METHODOLOGY

In this section, the proposed method is described, which mixes prior information and different types of ACMs, all balanced by the GDB. Furthermore, global weights regulate each term's contribution and are calculated through an optimization process.

2.1 Energy Terms

Let Ω be a bounded open subset of R^2, $I : [0, a] \times [0, b] \rightarrow R^+$ represents an image, and $C(q) : [0, 1] \rightarrow R^2$ is a parameterized planar curve in Ω. The curve C can be also implicitly represented via a Lipschitz function ϕ by $C = \{(x, y)|\phi(x, y) = 0\}$. C partitions Ω into the inside C set Ω_1 in which $\phi(x, y) > 0$, and the outside C set Ω_2 in which $\phi(x, y) < 0$.

2.1.1 Edge-based term

One of the most popular edge-based models is the Geodesic Active Contours model (GAC) [1]. Contour evolution occurs until strong edges are detected. The GAC model is formulated by minimizing the following energy functional:

$$E_{GAC}(C) = \int_0^1 g(|\nabla(I)(C(q))|)C'(q)|dq \qquad (1)$$

where g is an edge stopping function [1]. The g function regulates contour evolution, by terminating it when the contour faces strong edges. The Euler-Lagrange minimizer equation concludes to:

$$C_t = g(|\nabla(I)|)\kappa\vec{N} - (\nabla(g) \cdot \vec{N})\vec{N} \qquad (2)$$

where κ is the curvature of the contour and $\vec{N}$ is the inward normal to the curve C. A *baloon force* term is further added, in order to control the contour's evolution, through a constant velocity term α. Considering (1) and (2), the level set evolution formula reads:

$$\frac{\vartheta\phi}{\vartheta t} = g|\nabla(\phi)|(div(\frac{\nabla\phi}{|\nabla\phi|}) + \alpha) + \nabla g \cdot \nabla\phi \qquad (3)$$

2.1.2 Region-based term

The region-based model relies on statistical information of intensities, of the inner and outer regions of the evolving contour. The model used in this work is the well know Chan-Vese framework [2], which can be seen as a special case of the Mumford-Shah [10] problem. For a given image $I \in \Omega$, the Chan-Vese model is formulated by minimizing the following energy functional:

$$E_{CV} = \lambda_1 \int_{\Omega_1} |I(x, y) - c_1|^2 dxdy +$$

$$+\lambda_2 \int_{\Omega_2} |I(x, y) - c_2|^2 dxdy, \quad (x, y) \in \Omega \qquad (4)$$

where c_1 and c_2 are the average intensities of Ω_1 and Ω_2, respectively. Furthermore, augmenting the energy term with regularization terms of length and area, results to a smoother solution. By minimizing it, the corresponding variational level set formulation is obtained:

$$\frac{\vartheta\phi}{\vartheta t} = \delta_\epsilon(\phi)\left[\mu \operatorname{div}\left(\frac{\nabla\phi}{|\nabla\phi|}\right) - \nu - \lambda_1(I - c_1)^2 + \lambda_2(I - c_2)^2\right] \qquad (5)$$

where $\mu, \nu \geq 0$ control the smoothness and the evolution speed respectively, while $\lambda_1, \lambda_2 > 0$ control the image data driven force inside and outside C, respectively. δ_ϵ denotes the Dirac function.

2.1.3 Prior knowledge term

In an effort to model prior knowledge of the brain structures, a voxel-based statistical model is defined that captures knowledge on the spatial location of structures of interest.

Each labelled image L_n, $n = 1, \ldots, N$ is an image, with $L_n(v) = l$ for voxels v that belong to the l-th structure of interest and 0 otherwise.

The spatial distribution map L^l describes the empirical probability $p(l|v) \in [0, 1]$ for a given voxel v to have label l, i.e to belong to l-th structure of interest. Figure 2(a) shows $L^{hippocampus}$ in blue and $L^{amygdala}$ in red, with slightly purple being in the intermediate region.

The choice to model the prior information of the structure using the spatial distribution map has a great advantage, since it can be incorporated in the Chan-Vese model as a second input image. Given a contour that evolves in the image domain, L^l can be used in parallel in order to define the area that a contour is likely to evolve, based on the captured prior knowledge. The choice of utilizing the Chan-Vese model instead of the GAC, is becauseL^l has no high-gradient edges. The prior knowledge energy functional is:

$$E_{PR} = \mathtt{v}_1 \int_{\Omega_1} |L^l(x,y) - d_1|^2 dxdy + \\ + \mathtt{v}_2 \int_{\Omega_2} |L^l(x,y) - d_2|^2 dxdy, \quad (x,y) \in \Omega \qquad (6)$$

where d_1 and d_2 are now the probabilities of the regions inside and outside C and are calculated similarly with c_1 and c_2 while $\mathtt{v}_1$ and $\mathtt{v}_2$ correspond to λ_1 and λ_2. The level-set representation for the prior model, which minimizes equation (6) is the same with (5).

2.1.4 *Mixture of Energies*

Every brain structure has its own unique characteristics, having boundaries with varying gradient values, and inner regions with similar intensities with neighboring structures. A mixture approach combines different properties of the energy terms and mutually excludes disadvantages that in other ways would escalate bad performance and would lead to contour leak and false segmentation.

To enhance segmentation performance on boundary parts with strong gradients, the GAC model is used. However, if the target boundary is not well formed or contains weak-parts, the contour will leak to neighboring structures. In the challenging task of hippocampus and amygdala segmentation, hippocampus boundaries are strong along the structure except the neighboring boundary with the amygdala (figure 1). Due to this reason, the GAC model can perform well in the major area of the hippocampus, but will fail to detect the weaker boundary with amygdala. For amygdala, which has very weak boundaries everywhere, the GAC model seems to be totally inappropriate.

On the contrary, the Chan-Vese model has been widely used in applications that require segmentation on weak boundary objects. However, when intensities of neighboring, vaguely separated structures are of similar values (e.g. hippocampus and amygdala), the contour will continue to expand. To overcome this, a prior information term is mandatory to be included in the evolution process. The spatial distribution map can contribute, in order improve robustness and segmentation accuracy.

An experienced ratter would know beforehand that the lower and upper boundary of the hippocampus is well defined (figure 1), and thus would trust the image edges (GAC term), but in the region bordering with amygdala, would use its experience to conclude about the borders. In an effort to mimic the way the human expert will take advantage of his/her experience, the blending of the energy terms should be defined locally. This is GDB's role, as it tries to differentiate regions that need greater support of prior knowledge than these that can be segmented only by their gray-scale information. However, blending of these terms in the proposed methodology has to be done in accordance to segmentation accuracy and through a training procedure. Thus, the proposed blending scheme is given by:

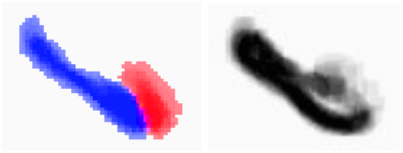

(a) (b)

Figure 2: (a) The spatial distribution map of hippocampus and amygdala. (b) Illustration of GDB, darker areas denote strong edge existence while lighter weak boundaries.

$$E_{TOTAL} = GDB \cdot (w_1 E_{GAC} + w_2 E_{CV}) + w_3 (1 - GDB) \cdot E_{PR} \quad (7)$$

Different values of the w_i weights will vary the segmentation performance. To find the ideal mix of w_i, based on the trained GDB, a global optimization method is required. Taking into account the solvers of E_{GAC}, E_{CV} and E_{PR}, the segmented structure will be determined by:

$$\frac{\vartheta \phi}{\vartheta t} = GDB \cdot (w_1 \phi_{GAC}^{upd} + w_2 \phi_{CV}^{upd}) + w_3 (1 - GDB) \cdot \phi_{PR}^{upd} \quad (8)$$

where ϕ_{GAC}^{upd} is given by (3), while ϕ_{CV}^{upd} and ϕ_{PR}^{upd} by (5).

2.2 Optimum Energy Mixing

In order to define GDB and $W = w_i$, based on prior knowledge, a training dataset is required. The GDB is based on image gradient information of MR images, while W is the result of an optimization procedure based on Particle Swarm Optimization (PSO).

2.2.1 *Gradient Distribution of Boundaries*

GDB has the same size and dimensionality with the MR image and acts as the balancer between the image term and the prior term. GDB's values define the extent to which one should trust the image information or the prior knowledge, at a voxel level [14]. Figure 2(b), shows GDB for the hippocampus-amygdala region, which reveals the inexistence of gradient values on the amygdala boundary, except for its lower-right region.

In order to build the GDB, the gradient magnitude on the perimeter of every structure is calculated. A thresholding operation is performed on the gradient values, which tries to connect neighboring pixels with similar gradient value and direction. This operation separates the boundary to its strong and weak gradient parts. In order to build a more generic map of gradient distribution, around the structure of interest, a morphological operator is applied to each pixel of the thresholded (binarized) image. The structure element's direction is always aligned with each pixel's normal unit, of the thresholded image and dilation is perfomed. The same procedure is applied to all MRI images of the training set

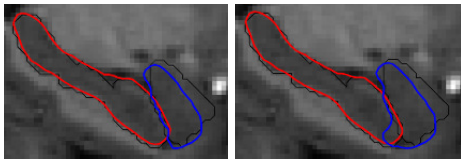

(a) (b)

Figure 3: (a) Segmentation outcome of the proposed model for amygdala (blue contour) and hippocampus (red contour). (b) Segmentation outcome without utilizing the repulsive term (overlapping occurs)

and the produced dilated images are averaged and normalized to $[0, 1]$.

2.2.2 *Weights Optimization*

In order to find the optimum W values, a variety of intelligent global optimizers could be applied, such as Artificial Neural Network, Simulated Annealing Algorithm, Ant Colony Optimization, Genetic Algorithms etc. In this work, Particle Swarm Optimization (PSO) [5] is used due to its low computational cost and its specialization in *Mixing Problems* like Ingredient Mix Optimization [6]. PSO tries to mimic the behavioral movement of swarms and flocks, as it happens in nature. An objective function is used to evaluate at each time, a group of candidate optimum solutions. Each candidate, is updated at each run in accordance with the best evaluated w_i in the swarm. At convergence, most of the particles will concentrate around the global optimum of the objective.

In this approach, the swarm consists of K weight vectors W_k, $k = 1...K$, where K is the swarm's population. The particles are evaluated against an objective function $f(W_k)$ that measures segmentation accuracy in the training set. The objective function used in the current analysis is the mean of averaged distance errors, between the segmentation result and the ground truth.

2.3 Multi-Structure Approach

Consider an image I that has M structures of interest $S_i, (i = 1, ..., M)$. Structures may be neighboring and in contact with each other, having unclear and weak boundaries, leading to leaked contours and oversegmentation. To deal with these problems, the use of L^l and GDB has been extended in a multiphase framework. Besides, overlapping is another problem that occurs when contours evolve independently, without any constraint in the interaction between them. In order to overcome this problem, a *coupling repulsive term* can be formulated, which ensures segmented structure independence and restrain contour conflicts for pixels that belong to marginal areas.

Each of the structures can follow the same training procedure of Section 2.2. Individual calculations of L^l, GDB and W for each structure, form its prior information profile.

2.3.1 *Modelling Structure Interaction*

A given contour C_i, which represents the segmented region S_i, should be allowed to evolve in a bounded domain in order not to interfere with other structures and avoid overlapping. To achieve this, a repulsive term is incorporated into the contour evolution update term which prevents the corresponding zero level set function ϕ_i to grow inside neighboring structures.

In an effort to formulate region ownership and competition, the Heaviside function H is used. Since the inner domain of level set functions contain negative values and the outer domain contains positive, $H(\phi_i)$ produces a binary mask for the exterior domain and $1 - H(\phi_i)$ corresponds to the interior domain, of S_i structure. Extending this idea to the initial intention to include coupling interaction between the structures in the image I domain and under the assumption that the structures are not initially overlapped, the R_i matrix is derived:

$$R_i = 1 - \sum_{j=1, j\neq i}^{N} (1 - H(\phi_j)) \tag{9}$$

R_i is the repulsive matrix for S_i structure and dynamically adjusts to C_i changes and their corresponding level-set functions ϕ_i. It represents the pixels which do not belong to $\{S_j\}$ structures, $j = 1..N, j \neq i$ and therefore formulates a dynamic label map for the allowed, non-conflicting bounded region (see figure 3 for the impact of repulsion term on segmenting amygdala and hippocampus).

In differential discrete analysis, the R_i matrix would be associated with equation (8), iteratively depending on dt time step and the *update term*, which is the right part of the aforementioned equation. To constrain the level set to the bounded domain, the update term is multiplied by the repulsive matrix R_i. R_i is calculated at each iteration, for each structure, along with the update term of (8).

$$\phi_i(t + 1) = \phi_i(t) + dt\phi_{update}(t) \cdot R_i \tag{10}$$

3. EXPERIMENTAL RESULTS

The proposed method was evaluated in the context of the leave-one-out procedure. For every excluded image, the GDB, the Spatial Distribution Map and the optimum weights are calculated, in an effort to evaluate the effectiveness of the energy mixing scheme. To compare the performance of the algorithm, results with the Chan-Vese model along with the prior information of spatial distribution map are presented. Furthermore, the optimum global weights are given to explain the significance of each term's presence in the scheme.

3.1 Evaluation Dataset

The proposed methodology has been tested on 13 MR T1 weighted MP-RAGE images, randomly chosen from the OASIS database [9]. A professional radiologist manually traced the hippocampus and amygdala volume on those 13 images, in order to build the labelled image training set. Apart from OASIS pre-processing, the selected MR images were further rigidly registered on the hippocampus-amygdala complex's center of mass. The dataset used in the experiments consists of the central sagittal slices of the complex, one taken from each MRI.

3.2 Comparisons

As showed in [14], selecting initial seeds from the high probable voxels of the spatial distribution map, boosts the performance, by offering a reliable initialization to the segmentation procedure. The performance of the algorithm is evaluated by different metrics that define either distance errors or precision-recall accuracy. Figure 3.2 presents the

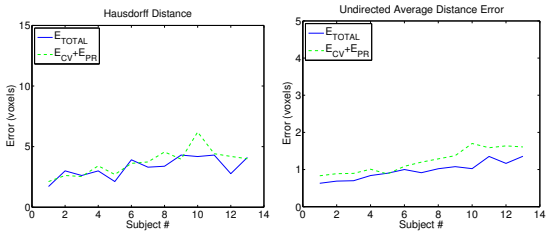

(a) (b)

Figure 4: Comparisons based on (a) the Haussdorf distance, and (b) the undirected averaged distance.

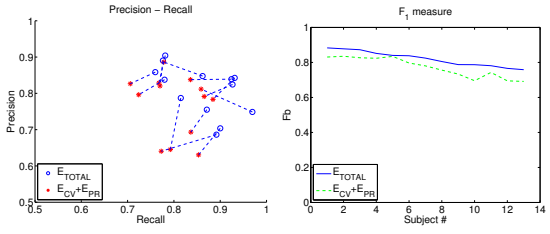

(a) (b)

Figure 5: Comparisons based on Precision vs Recall diagrams and the F_1/Dice coefficient. In (a) results of the two compared methods on the same image are connected with dashed lines to highlight the improvement of the proposed method.

Haussdorf distance and the undirected averaged distance error, while in figure 3.2, Precision vs Recall metrics and F_1 measure are illustrated.

As can be seen by the evaluation metrics (see table 3.2), the majority of the test cases were significantly improved by the proposed scheme. Overall, leakage is diminished and the interaction model successfully constraints overlapping. In table 3.2, the optimized weights are presented for each of the tested structure. As expected, the GAC model has major influence in the hippocampus segmentation, since hippocampus actually has a significant portion of strong boundaries. The weights of amydgala reveal the fact that there are not enough gradients on its boundary to trust for its segmentation. Further, in both cases prior knowledge seemed to offer significant help. In order to fully understand the significance of each term and the balance among the image terms and the prior term, one should keep in mind that these weights are further weighted by the GVM.

Table 1: Averaged Comparison Results for HC-AM

	F_1	Prec.	Recall	Haus.	Avrg Dst
E_{TOTAL}	0.81	0.81	0.86	3.28	0.97
$E_{CV} + E_{PR}$	0.77	0.77	0.80	3.69	1.22

4. CONCLUSIONS

The proposed method tries to optimally blend image terms with prior information in a sophisticated local and global weighting scheme, in order to segment multiple objects simultaneously. GDB locally influences the contour evolution, depending on each structure's unique boundary characteristics, while global weights establish a general balance between the energy terms. Experimental results verified that the proposed framework's enhanced performance.

Table 2: Averaged optimum weights W

	GAC	C-V	Prior
HC	0.40	0.37	0.23
AM	0.11	0.74	0.15

5. ACKNOWLEDGMENTS

The authors would like to thank the OASIS team for providing their dataset and to give special thanks to Angelos Baltatzidis M.D., Radiologist for building the training set by performing the manual segmentations of hippocampus and amygdala.

6. REFERENCES

[1] V. Caselles, R. Kimmel, G. Sapiro, "Geodesic active contours", International Journal of Computer Vision, 22(1), 61-79, 1997.

[2] T. Chan and L. Vese, "Active contours without edges", IEEE Trans. Image Processing, vol. 10, pp. 266-277, 2001.

[3] T. F. Cootes, C. J. Taylor, D. H. Cooper, and J. Graham, "Active shape models-Their training and application", Com. Vis. Image Understand, vol. 61, Jan. 1995.

[4] C. Davatzikos, X. Tao, and D. Shen, "Hierarchical active shape models, using the wavelet transform", IEEE Trans. on Medical Imaging, vol 22, no 3, 2003.

[5] J. Kennedy, R. Eberhart, "Particle swarm optimization", IEEE conf. on Neural Networks, pp. 1942-1948 vol.4, 1995

[6] J. Kennedy, C. Russel, C. Erberhart, S. Yuhui, "Swarm Intelligence", Academic Press, San Diego, USA, 2001.

[7] J. M. Leventon, E. Grimson, and O. Faugeras, "Statistical shape influence in geodesic active contours", in Proc. IEEE Conf. Comp. Vision Pattern Recognition, 2000.

[8] A. Litvin and W. C. Karl, "Coupled shape distribution-based segmentation of multiple objects," in Proc. Inform. Process. Med. Imag., pp. 345-356, 2005.

[9] D.S. Marcus, T.H. Wang, J. Parker, J.G. Csernansky, J.C. Morris, and R.L. Buckner, "Open Access Series of Imaging Studies (OASIS): Cross-Sectional MRI Data in Young, Middle Aged, Nondemented, and Demented Older Adults", Journal of Cognitive Neuroscience, 19, 1498-1507.

[10] D. Mumford, J. Shah, "Optimal approximation by piecewise smooth function and associated variational problems", Communication on Pure and Applied Mathematics 42, pp. 577-685, 1989.

[11] A. Tsai, W. Wells, C. Tempany, E. Grimson, and A. Willsky, "Mutual information in coupled multi-shapemodel for medical image segmentation", Med. Image Anal., vol. 8, no. 4, pp. 429-445, 2004.

[12] P. Yan, A. Kassim, W. Shen and M. Shah, "Modeling Interaction for Segmentation of Neighboring Structures", IEEE Transactions on Information Technology in Biomedicine, vol. 13, No. 2, March 2009.

[13] J. Yang, L.H. Staib and J.S. Duncan, "Neighbor Constrained Segmentation with Level Set Based 3D Deformable Models", IEEE Trans. on Medical Imaging, vol. 23(8), 2004.

[14] D. Zarpalas, A. Zafeiropoulos, P. Daras and N. Maglaveras, "Hippocampus Segmentation using a Local Prior Model on its Boundary", International Conference on Machine Vision, Image Processing and Pattern Analysis, Venice, 2011.